

Formation of the black-hole binary M33 X-7 through mass exchange in a tight massive system

Francesca Valsecchi¹, Evert Glebbeek², Will M. Farr¹, Tassos Fragos^{1,5}, Bart Willems¹, Jerome A. Orosz³, Jifeng Liu^{4,5} & Vassiliki Kalogera¹

The X-ray source M33 X-7 in the nearby galaxy Messier 33 is among the most massive X-ray binary stellar systems known, hosting a rapidly spinning, $15.65M_{\odot}$ black hole orbiting an underluminous, $70M_{\odot}$ main-sequence companion in a slightly eccentric 3.45-day orbit^{1,2} (M_{\odot} , solar mass). Although post-main-sequence mass transfer explains the masses and tight orbit³, it leaves unexplained the observed X-ray luminosity, the star's underluminosity, the black hole's spin and the orbital eccentricity. A common envelope phase¹, or rotational mixing⁴, could explain the orbit, but the former would lead to a merger and the latter to an overluminous companion. A merger would also ensue if mass transfer to the black hole were invoked for its spin-up⁵. Here we report simulations of evolutionary tracks which reveal that if M33 X-7 started as a primary body of $85M_{\odot}$ – $99M_{\odot}$ and a secondary body of $28M_{\odot}$ – $32M_{\odot}$, in a 2.8–3.1-d orbit, its observed properties can be consistently explained. In this model, the main-sequence primary transfers part of its envelope to the secondary and loses the rest in a wind; it ends its life as a $\sim 16M_{\odot}$ helium star with an iron–nickel core that collapses to a black hole (with or without an accompanying supernova). The release of binding energy, and possibly collapse asymmetries, 'kick' the nascent black hole into an eccentric orbit. Wind accretion explains the X-ray luminosity, and the black-hole spin can be natal.

M33 X-7 has been identified as an evolutionary challenge, given the massive components and the tight orbit of the system relative to the size of the large hydrogen-rich companion. Four mechanisms have been proposed to explain the formation of M33 X-7, but none of them has

addressed nor can simultaneously explain all its observed properties (Tables 1 and 2). We performed detailed binary evolution calculations to explore possible evolutionary tracks. Given the spatial metallicity gradient of Messier 33⁶ (M33) we assume a metallicity of 50% of the solar value for all our models.

To illustrate the evolutionary history of M33 X-7 clearly, we show the results for one of the successful evolutionary sequences in Fig. 1. The binary progenitor comprises a primary of $\sim 97M_{\odot}$ (the progenitor of the black hole) and a secondary of $\sim 32M_{\odot}$ (the progenitor of the black-hole companion) in an orbit of ~ 2.9 d. During the first ~ 1.8 Myr, the evolution is driven by mass loss due to stellar winds, causing a decrease in the gravitational attraction between the components and the increase of the orbit to ~ 3.25 d. The more massive primary evolves faster than the secondary, growing in size to accommodate the energy produced by fusing hydrogen into helium at its centre. Eventually, while still on the main sequence, it expands and begins mass transfer to the secondary when it enters the sphere of influence of the secondary's gravitational field (through Roche-lobe overflow). This stronger mode of mass loss brings the primary out of thermal equilibrium; in response, the star shrinks, recovering its thermal equilibrium while always maintaining hydrostatic equilibrium and, hence, dynamical stability. During the first few tens of thousands of years of mass transfer, the orbital period decreases because the more massive primary is transferring mass to the less massive secondary. When the secondary accretes enough matter to become the more massive component, the orbit starts expanding⁷. The primary transfers most of its hydrogen-rich envelope and becomes a Wolf–Rayet star, and the strong Wolf–Rayet wind ($\sim (2\text{--}3) \times 10^{-5}M_{\odot} \text{ yr}^{-1}$) removes much

Table 1 | Observed parameters for M33 X-7 for the reference distance of 840 ± 20 kpc adopted by the discovery team¹

Parameter	Value
M_{BH}	$15.65M_{\odot} \pm 1.45M_{\odot}$
M_2	$70.0M_{\odot} \pm 6.9M_{\odot}$
Spectral type	O7III to O8III
T_{eff}	$35,000 \pm 1,000$ K
$\text{Log}(L_2/L_{\odot})$	5.72 ± 0.07
P	3.45301 ± 0.00002 d
e	0.0185 ± 0.0077
i	$74.6 \pm 1.0^{\circ}$
L_X	$(0.13\text{--}2.49) \times 10^{38} \text{ erg s}^{-1}$
a^*	0.84 ± 0.05

The black-hole mass (M_{BH}), the mass (M_2), spectral type, effective temperature (T_{eff}) and luminosity (L_2) of its companion, the orbital eccentricity (e) and the inclination (i) are as reported in ref. 1. The orbital period (P) is as measured in ref. 2. The dimensionless spin parameter of the black hole (a^*) was determined in ref. 9 on the basis of the X-ray continuum fitting method^{16–18}. The X-ray luminosity (L_X) is derived from observations reported in refs 1, 2, 9, 19–21. To account for variations in the X-ray flux over different observations, we consider the lowest and highest reported values, after we rescale each L_X to an M33 distance of 840 ± 20 kpc. If the full distance range of 750–1,017 kpc is adopted, using the ELC code of ref. 22 we calculate the masses to be $55M_{\odot}$ – $103M_{\odot}$ and $13.5M_{\odot}$ – $20M_{\odot}$ for the star and the black hole, respectively, and the inclination is 77° – 71° . The logarithmic luminosity in solar units is then 5.62–5.89 (ref. 1). For each distance, the mass of the star can be derived from $M_2 = -75.94 + 0.17d$ and the inclination from $i = 93.69 - 0.02d$, where d is in kiloparsecs, M_2 is in solar masses and i is in degrees. For each M_2 , the corresponding black hole's mass in solar masses can be calculated from $M_{\text{BH}} = 6.19 + 0.13M_2$, and its spin can be calculated from $a^* = 0.31 + 0.049M_{\text{BH}} - 0.001M_{\text{BH}}^2$. The rescaled X-ray luminosity ranges from $\sim 1 \times 10^{37}$ to $\sim 3 \times 10^{38} \text{ erg s}^{-1}$.

Table 2 | Models suggested for the formation of M33 X-7

Model	M_{BH}	M_2	T_{eff}	$\text{Log}(L_2)$	P	e	L_X	a^*
Ref. 1	X	O	O	O	X	O	X	O
Ref. 3	✓	✓	O	O	✓	O	O	O
Ref. 4	X	X	O	O	X	O	O	O
Ref. 5	O	O	O	O	O	O	O	✓

The various parameters are described in Table 1. The symbol '✓' means a parameter has been addressed and explained, 'X' means a parameter has been addressed but not explained and 'O' means a parameter has not been addressed at all. To explain the tight orbit, ref. 1 suggests that the progenitors underwent a common envelope phase during which the primary expanded to the point of engulfing its companion. Such a phase is known to produce tight systems because energy can be transferred from the orbit to the common envelope, leading to a reduction in the binary separation and ejection of the envelope²³. To form the observed black hole, ref. 1 requires that the common envelope begins after helium core burning in the primary is complete. However, a common envelope in the case of M33 X-7 would probably evolve into a merger, because massive-star envelopes are tightly bound²⁴. Furthermore, for this model to succeed an unrealistically low stellar wind would be required. Ref. 3 suggests a phase of conservative mass transfer from the black-hole progenitor to the companion that sets in when the primary leaves the main sequence, but this model only explains the observed masses and orbital period, and fails to address the remaining observations. Ref. 4 proposes rotationally induced mixing as a way to keep massive stars from expanding significantly during the main sequence, preventing mass transfer or a merger until the primary becomes a Wolf–Rayet star. However, this evolutionary channel increases the star's luminosity above that of standard models, which contradicts the observed underluminosity of the star in M33 X-7. Ref. 5 explains the observed black hole's spin in terms of a past Roche-lobe overflow phase from the star to the black hole. However, given the extreme mass ratio between the components, such a phase would have evolved into a merger.

¹Center for Interdisciplinary Exploration and Research in Astrophysics (CIERA) and Department of Physics and Astronomy, Northwestern University, 2145 Sheridan Road, Evanston, Illinois 60208, USA. ²Department of Physics and Astronomy, McMaster University, 1280 Main Street West, Hamilton, Ontario L8S 4M1, Canada. ³Department of Astronomy, San Diego State University, 5500 Campanile Drive, San Diego, California 92182-1221, USA. ⁴National Astronomical Observatories, Chinese Academy of Sciences, Beijing 100012, China. ⁵Harvard-Smithsonian Center for Astrophysics, 60 Garden Street, Cambridge, Massachusetts 02138, USA.

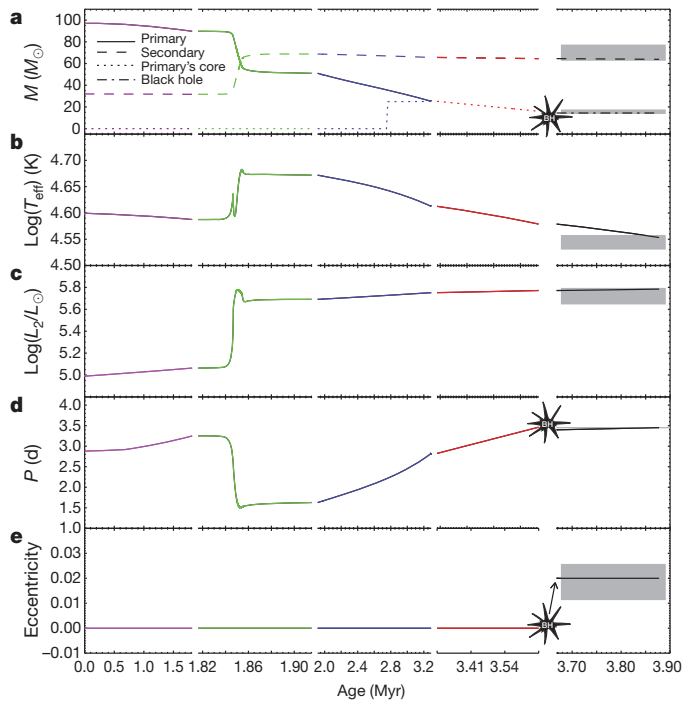


Figure 1 | Evolution of the orbital and stellar parameters of M33 X-7. **a**, Masses (M); **b**, secondary's surface temperature ($\log(T_{\text{eff}})$); **c**, secondary's luminosity ($\log(L_2)$); **d**, orbital period (P); **e**, eccentricity (e). The different evolutionary stages are highlighted with different colours: the beginning of the main sequence, purple; the mass transfer phase, green; the end of the main sequence, blue; the core helium burning phase for the black-hole progenitor, red; the phase between black-hole formation and the present time, black. (Note the non-uniform x axis.) The grey shaded areas represent the observational constraints as reported in Table 1. The sequence comprises an $M_1 \approx 97M_\odot$ primary and an $M_2 \approx 32M_\odot$ secondary in a ~ 2.9 -d orbit. At the onset of the mass transfer phase (purple/green), $M_1 \approx 89.7M_\odot$, $M_2 \approx 31.7M_\odot$ and $P \approx 3.25$ d. During the mass transfer phase (green), the primary transfers conservatively $\sim 37M_\odot$ to the companion (see Supplementary Information for details about the mass transfer). When the system detaches (green/blue), $M_1 \approx 51M_\odot$, $M_2 \approx 68.7M_\odot$ and $P \approx 1.6$ d. When the primary leaves the main sequence (blue/red), $M_1 \approx 25.2M_\odot$, $M_2 \approx 65.6M_\odot$ and $P \approx 2.8$ d. Considering evolutionary models of helium stars (Supplementary Information), we find that a helium star of $\sim 25M_\odot$ burns helium at its centre for ~ 0.38 Myr and loses $\sim 9.1M_\odot$ to its Wolf-Rayet wind. During this time (red), the secondary loses $\sim 1.1M_\odot$. Before black-hole formation (red/black), $M_1 \approx 16M_\odot$, $M_2 \approx 64.5M_\odot$ and $P \approx 3.46$ d. For the case shown, at the primary's collapse a kick of 120 km s^{-1} is imparted to the newly formed black hole (see Supplementary Information for the allowed kicks).

of the remaining envelope, eventually interrupting the mass transfer. During the ~ 99 kyr of conservative mass transfer, the original $32M_\odot$ secondary becomes a massive, $\sim 69M_\odot$ O-type star and the primary becomes a $\sim 51M_\odot$ Wolf-Rayet star. Once the Wolf-Rayet wind begins and the mass transfer is interrupted, the wind blows away the remaining primary's envelope to expose the $\sim 25M_\odot$ helium core. This mass loss drives further orbital expansion until the primary leaves the main sequence and throughout the phase of core helium burning. At the same time, the secondary, which is now more massive, is losing mass to its own O-star wind at a lower rate ($\sim 10^{-6}M_\odot \text{ yr}^{-1}$). At this time, the orbit of the binary is circular and the spin period of each star is expected to be synchronized with the orbital period. The synchronization is due to exchange of angular momentum between the stars and their orbit, caused by tidal interaction.

The final stages of the primary's life during and after carbon burning are too short (~ 60 yr for an initially $\sim 25M_\odot$ helium star⁸) to change the stellar and orbital parameters significantly. At the end of the primary's life, after ~ 3.7 Myr, M33 X-7 comprises a $\sim 16M_\odot$, evolved Wolf-Rayet star with an iron-nickel core and a $\sim 64.5M_\odot$ O-star companion in a

~ 3.5 -d orbit. Unable to support itself through further nuclear fusion, this massive, helium-rich star collapses into a black hole and a small fraction of the rest-mass energy (10%) is released as the black hole's gravitational energy. Additionally, asymmetries in the collapse and associated neutrino emission may impart an instantaneous linear momentum recoil (kick) to the newly born black hole, even if there is no baryonic mass ejection at collapse. Both of these effects modify the orbital configuration, inducing an eccentricity and slightly decreasing the orbital period to ~ 3.4 d. The release in binding energy leads to an increase in the orbital separation and the kick imparted to the black hole acts to decrease it. For the ~ 0.2 Myr after the formation of the black hole, the binary evolution is driven by mass loss due to the secondary's stellar wind, causing the orbit to expand further, to the currently observed value. The fraction of this stellar wind attracted and accreted by the black hole is too small to influence the orbital evolution significantly, but is adequate to explain the X-ray luminosity observed. Today, after ~ 3.9 Myr, M33 X-7 comprises a black hole of $\sim 14.4M_\odot$ and an underluminous O star of $\sim 64M_\odot$ orbiting around their common centre of mass in a slightly eccentric, ~ 3.45 -d orbit.

Our model is consistent with a natal nature of the black hole's observationally inferred high spin⁹. In fact, although it has been suggested that such a high spin is the result of a mass transfer from the companion star to the black hole through Roche-lobe overflow⁵, given how much more massive the companion is relative to the black hole, such a phase could not have occurred: the mass transfer would have been dynamically unstable and would have rapidly evolved into a merger of the binary components. Wind accretion is too weak to spin up the black hole to the current value if it had been formed spinning much slower. In our model, when the black-hole progenitor leaves the main sequence, the spins of the stars are expected to be synchronized with the orbit, and, assuming rigid-body rotation on the main sequence, the inner parts of the primary's core carry enough angular momentum to explain the currently observed black-hole spin (the inner $15.5M_\odot$ of the core carry $\sim 5.2 \times 10^{51} \text{ g cm}^2 \text{ s}^{-1}$ of angular momentum, and $\sim 1.8 \times 10^{51} \text{ g cm}^2 \text{ s}^{-1}$ is needed to explain the currently observed spin). At the end of the main sequence, the inner core of the star is expected to decouple rotationally from the outer envelope and approximately retain the angular momentum of the central layers (see table 4 in ref. 10).

We explore binary evolutionary sequences with different combinations of initial masses and orbital periods. We select as 'successful' sequences those that eventually match all observed properties within 1σ errors. All these sequences follow a path qualitatively very similar to the specific example described in detail here. The progenitors are constrained to host $96M_\odot$ – $99M_\odot$ primaries and $32M_\odot \pm 1M_\odot$ secondaries in orbits with initial periods of 2.8–2.9 d. The apparent puzzling underluminosity of the black-hole companion is due to two factors: the orientation of the system with respect to our line of sight and associated projection effects reduce the star's measured luminosity (accounting for 87% of the underluminosity), and the secondary was not formed as a $\sim 63M_\odot$ – $65M_\odot$ star but instead accreted much of its mass (accounting for 13% of the underluminosity) from the black-hole progenitor (Supplementary Information).

We note that the uncertainty in the distance to M33, ~ 840 kpc, is greater than ± 20 kpc, and that some of the observed system properties vary if a different distance to the system is considered (Table 1). Various studies in the literature have reported the distance to be in the range 750–1,017 kpc (Supplementary Information). Considering this full range, the progenitors are constrained to host primaries of $85M_\odot$ – $99M_\odot$, secondaries of $28M_\odot$ – $32M_\odot$ and initial orbital periods of 2.8–3.1 d (Fig. 2).

The different phases we have described for the evolutionary past of M33 X-7 have been observed in a variety of other binary systems. For example, the super star cluster R136 in the Large Magellanic Cloud hosts two non-interacting O stars of $\sim 57M_\odot$ and $\sim 23M_\odot$ orbiting around each other every ~ 3.4 d (LMC R136-38, ref. 11). The eclipsing

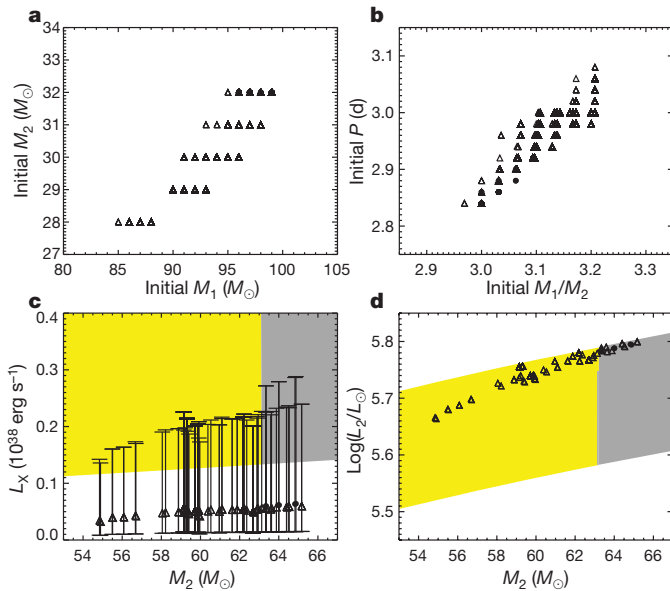


Figure 2 | Progenitor properties and current luminosity. Data represented by circles and triangles are the results of detailed binary star evolution calculations for all successful sequences for M33 distances of 840 ± 20 kpc and $750\text{--}1,017$ kpc, respectively. **a**, Possible masses for the progenitors; **b**, possible initial orbital periods as a function of the mass ratio between the primary and the secondary; **c**, **d**, black-hole X-ray luminosity (**c**) and secondary's luminosity (**d**) as functions of the secondary's mass at present. The grey and yellow shaded areas represent the observational constraints for M33 distances of 840 ± 20 kpc and $750\text{--}1,017$ kpc, respectively. L_X is calculated according to the Bondi–Hoyle accretion model²⁵. The error bars are derived from the uncertainties in the stellar wind parameters (Supplementary Information) and depict the highest and lowest L_X values; they do not represent statistical 1σ errors. The observational constraints on L_2 are calculated given the dependence of M_2 and L_2 on the distance as described in the caption of Table 1, and accounting for uncertainties in the star's effective temperature, reddening and apparent magnitude calculated using the ELC code²². According to our model, secondaries at present more massive than $\sim 65M_\odot$ fail to explain the observed luminosity. Some of the data points are omitted for clarity.

binary LMC-SC1-105 comprises a $\sim 31M_\odot$ O star that is transferring mass to its $\sim 13M_\odot$ companion¹². In the system WR46, a $\sim 51M_\odot$ Wolf–Rayet star orbits a $\sim 60M_\odot$ O-star companion every ~ 6 d. In particular, the various discoveries of Wolf–Rayet stars with O-star companions¹³ validate our theoretical model, as they resemble the configuration of M33 X-7 less than 2 Myr ago. Several of these binaries have been observed with orbital periods of a few days and massive components^{14,15} (up to $\sim 80M_\odot$).

Received 22 December 2009; accepted 26 August 2010.

Published online 20 October 2010.

- Orosz, J. A. *et al.* A 15.65-solar-mass black hole in an eclipsing binary in the nearby spiral galaxy M 33. *Nature* **449**, 872–875 (2007).
- Pietsch, W. *et al.* M33 X-7: ChASeM33 reveals the first eclipsing black hole X-ray binary. *Astrophys. J.* **646**, 420–428 (2006).
- Abubekrov, M. K., Antokhina, E. A., Bogomazov, A. I. & Cherepashchuk, A. M. The mass of the black hole in the X-ray binary M33 X-7 and the evolutionary status of M33 X-7 and IC 10 X-1. *Astron. Rep.* **53**, 232–242 (2009).

- de Mink, S. E. *et al.* Rotational mixing in massive binaries. Detached short-period systems. *Astron. Astrophys.* **497**, 243–253 (2009).
- Moreno Méndez, E., Brown, G. E., Lee, C. & Park, I. H. The case for hypercritical accretion in M33 X-7. *Astrophys. J.* **689**, L9–L12 (2008).
- Vivian, U. *et al.* A new distance to M33 using blue supergiants and the FGLR method. *Astrophys. J.* **704**, 1120–1134 (2009).
- Verbunt, F. Origin and evolution of X-ray binaries and binary radio pulsars. *Annu. Rev. Astron. Astrophys.* **31**, 93–127 (1993).
- Tauris, T. M. & van den Heuvel, E. in *Compact Stellar X-Ray Sources* (eds Lewin, W. & van der Klis, M.) 623–665 (Cambridge Univ. Press, 2006).
- Liu, J., McClintock, J. E., Narayan, R., Davis, S. W. & Orosz, J. A. Erratum: “Precise measurement of the spin parameter of the stellar-mass black hole M33 X-7”. *Astrophys. J.* **719**, L109 (2010).
- Hirschi, R., Meynet, G. & Maeder, A. Stellar evolution with rotation. XIII. Predicted GRB rates at various Z . *Astron. Astrophys.* **443**, 581–591 (2005).
- Massey, P., Penny, L. R. & Vukovich, J. Orbits of four very massive binaries in the R136 cluster. *Astrophys. J.* **565**, 982–993 (2002).
- Bonanos, A. Z. Toward an accurate determination of parameters for very massive stars: the eclipsing binary LMC-SC1–105. *Astrophys. J.* **691**, 407–417 (2009).
- van der Hucht, K. A. The VIIth catalogue of galactic Wolf–Rayet stars. *N. Astron. Rev.* **45**, 135–232 (2001).
- Rauw, G. *et al.* WR 20a: a massive cornerstone binary system comprising two extreme early-type stars. *Astron. Astrophys.* **420**, L9–L13 (2004).
- Bonanos, A. Z. *et al.* WR 20a is an eclipsing binary: accurate determination of parameters for an extremely massive Wolf–Rayet system. *Astrophys. J.* **611**, L33–L36 (2004).
- Zhang, S. N., Cui, W. & Chen, W. Black hole spin in X-ray binaries: observational consequences. *Astrophys. J.* **482**, L155–L158 (1997).
- Li, L., Zimmerman, E. R., Narayan, R. & McClintock, J. E. Multitemperature blackbody spectrum of a thin accretion disk around a Kerr black hole: model computations and comparison with observations. *Astrophys. J. Suppl. Ser.* **157**, 335–370 (2005).
- McClintock, J. E. *et al.* The spin of the near-extreme Kerr black hole GRS 1915+105. *Astrophys. J.* **652**, 518–539 (2006).
- Parmar, A. N. *et al.* BeppoSAX spectroscopy of the luminous X-ray sources in M 33. *Astron. Astrophys.* **368**, 420–430 (2001).
- Pietsch, W. *et al.* The eclipsing massive X-ray binary M 33 X-7: new X-ray observations and optical identification. *Astron. Astrophys.* **413**, 879–887 (2004).
- Taam, R. E. & Sandquist, E. L. Common envelope evolution of massive binary stars. *Annu. Rev. Astron. Astrophys.* **38**, 113–141 (2000).
- Podsiadlowski, P., Rappaport, S. & Han, Z. On the formation and evolution of black hole binaries. *Mon. Not. R. Astron. Soc.* **341**, 385–404 (2003).
- Bondi, H. & Hoyle, F. On the mechanism of accretion by stars. *Mon. Not. R. Astron. Soc.* **104**, 273–282 (1944).

Supplementary Information is linked to the online version of the paper at www.nature.com/nature.

Acknowledgements We thank N. Ivanova, A. Heger, A. Cantrell and C. Bailyn for discussions during the development of this project.

Author Contributions V.K. and B.W. designed the study. F.V. led the project, performed the single and binary star evolution calculations, and developed the code to perform the orbital evolution after black-hole formation. V.K. and B.W. collaborated with F.V. in each step of the project. E.G. maintained, updated and extended the stellar evolution code used, and collaborated with F.V. in performing the calculations. W.M.F. determined the correction to the star's luminosity and surface temperature due to the inclination of the system. T.F. led the theoretical analysis of the black-hole spin. J.A.O. performed the analysis of the observational data on M33 X-7 using the ELC code for the full distance uncertainty. J.L. recalculated the black hole's spin at different distances. All authors discussed the results and made substantial contributions to the manuscript.

Author Information Reprints and permissions information is available at www.nature.com/reprints. The authors declare no competing financial interests. Readers are welcome to comment on the online version of this article at www.nature.com/nature. Correspondence and requests for materials should be addressed to F.V. (francesca@u.northwestern.edu).